Satellite-Derived Resource Assessment in Afghanistan & Pakistan in support of the USAID South Asia Regional Initiative

Prepared by

Richard Perez
Jim Schlemmer
Kathleen Moore
Ray George

NREL subcontract # AEJ65517201
David Renné, Project Manager

FINAL REPORT

Satellite-Derived Resource Assessment in Afghanistan & Pakistan in support of the USAID South Asia Regional Initiative

Prepared by

Richard Perez
Jim Schlemmer
Kathleen Moore
Ray George

NREL subcontract # AEJ65517201
David Renné, Project Manager

FINAL REPORT

OBJECTIVE

The objective of the project is to produce high resolution satellite-derived global and direct irradiance data for the countries of Afghanistan and Pakistan. Data products include hourly time series and monthly averages spanning three years for each high resolution point.

This high resolution irradiance information constitutes one of the inputs tot the Geographic Information System (GIS) tools and packages developed by NREL for the region, and providing interactive solar, wind, hydro and biomass resources information.

METHODOLOGY

Acquisition of Satellite and other model input data

Satellite Data: The geostationary satellite covering the region is the European satellite Meteosat 5. This satellite is currently positioned at a longitude of 63^{o} after initial service at 0^{o} longitude. Its current position provides a very good vantage point for the Afghanistan-Pakistan region, with a field of view comparable to that of the US GOES-East satellite for the southeastern US.

Hourly visible satellite images constitute the primary input to the SUNY model [1, 2]. We purchased and received three years of hourly Meteosat 5 visible-channel area files from University of Wisconsin's McIdas group, covering a period from May 1st, 2002 to September 8th, 2005. From the McIdas area files, we built an archive gridded on a constant latitude-longitude mesh (0.1^{o}) analogous to our operational US GOES-based archive. As part of this process, we visually inspected all hourly frames to flag corrupted images. An example of a gridded image in the operational archive is shown in Figure 1 -- note the snow-capped Himalayas (top right) and the coastline of Pakistan (bottom left).

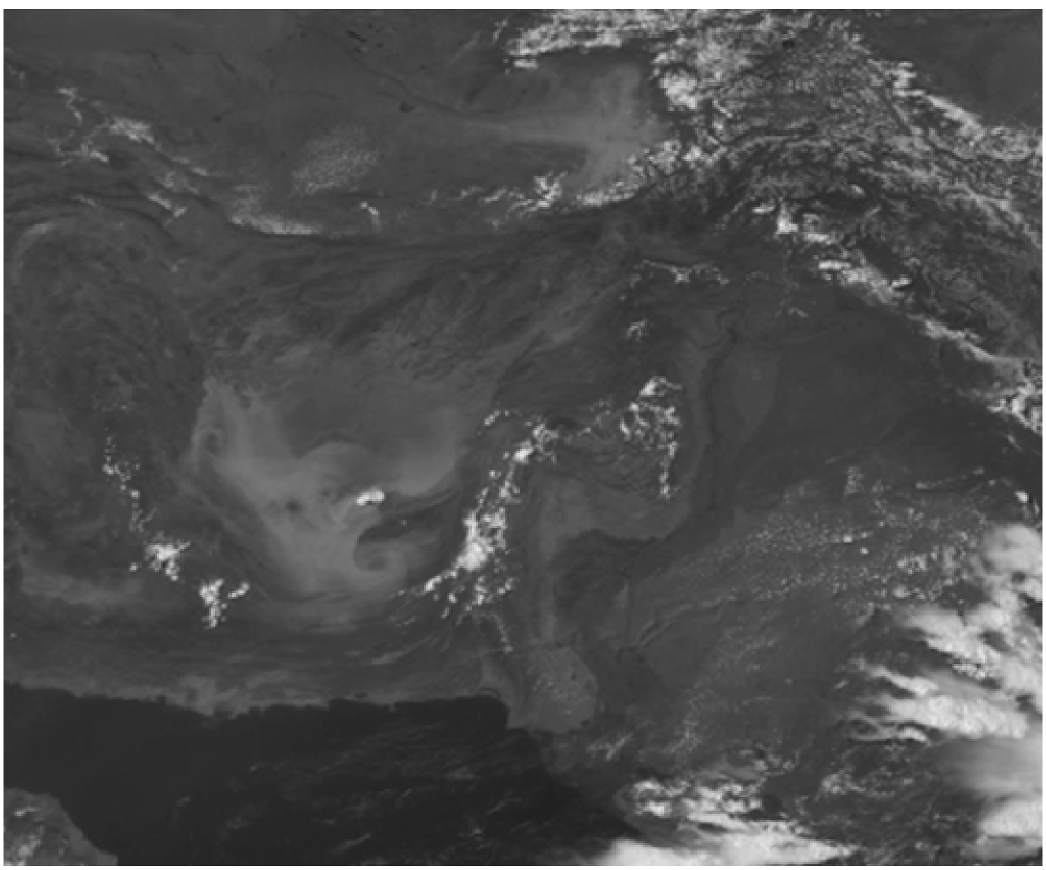

Figure 1: *Sample visible channel frame gridded on a constant latitude-longitude mesh and used as operational input to the SUNY model.*

In addition to visible–channel satellite data, the SUNY model requires gridded monthly climatological means for precipitable water, stratospheric ozone, and broad-band atmospheric optical depth (AOD), as well as daily snow cover data, and terrain elevation data.

<u>AOD and precipitable water data</u>: Monthly climatological averages of gridded precipitable water (W) and broad band optical depth were received from Ray George, along with gridded terrain elevation data. These data are equivalent to that used in NREL's CSR model [8].

<u>Ozone data</u>: Monthly climatological averages of stratospheric ozone had been previously made available to us by NREL for the considered latitudes.

<u>Snow cover data</u>: Kathleen Moore of Integrated Environment Data was contracted to produce gridded daily snow cover data from the NOAA-NESDIS archives. The gridded daily snow cover data for the region were generated by geo-referencing and scanning the snow-cover maps available from the NOAA NESDIS archive [3].

All data archives have the same ground resolution: 0.1 degree latitude by 0.1 degree longitude, amounting to approximately 8.5 x 10 km in the considered region.

Adapting the SUNY satellite model to Meteosat

The SUNY model was initially based on a model developed for Meteosat by Zelenka [4], which was itself based on the Heliosat-1 methodology [5]. However, it has evolved considerably over the years and all the new developments have been directed to modeling GOES data.

<u>Satellite data preprocessing</u>: Our first step in this process was to detect whether images received from U. Wisconsin-McIdas [6] had been altered for better visualization – for the GOES satellites, McIdas routinely applies a square root filter to image pixels that must be removed prior to modeling. Reviewing data samples for multiple locations and observing trends, we concluded that the Meteosat data had not been processed for better visualization. Indeed, unlike for GOES, the image pixel counts are linearly proportional to the observed earth's radiance. Figure 2 compares the zenith angle signature of a GOES pixel and a Meteosat pixel at one of the many locations investigated for this exercise.

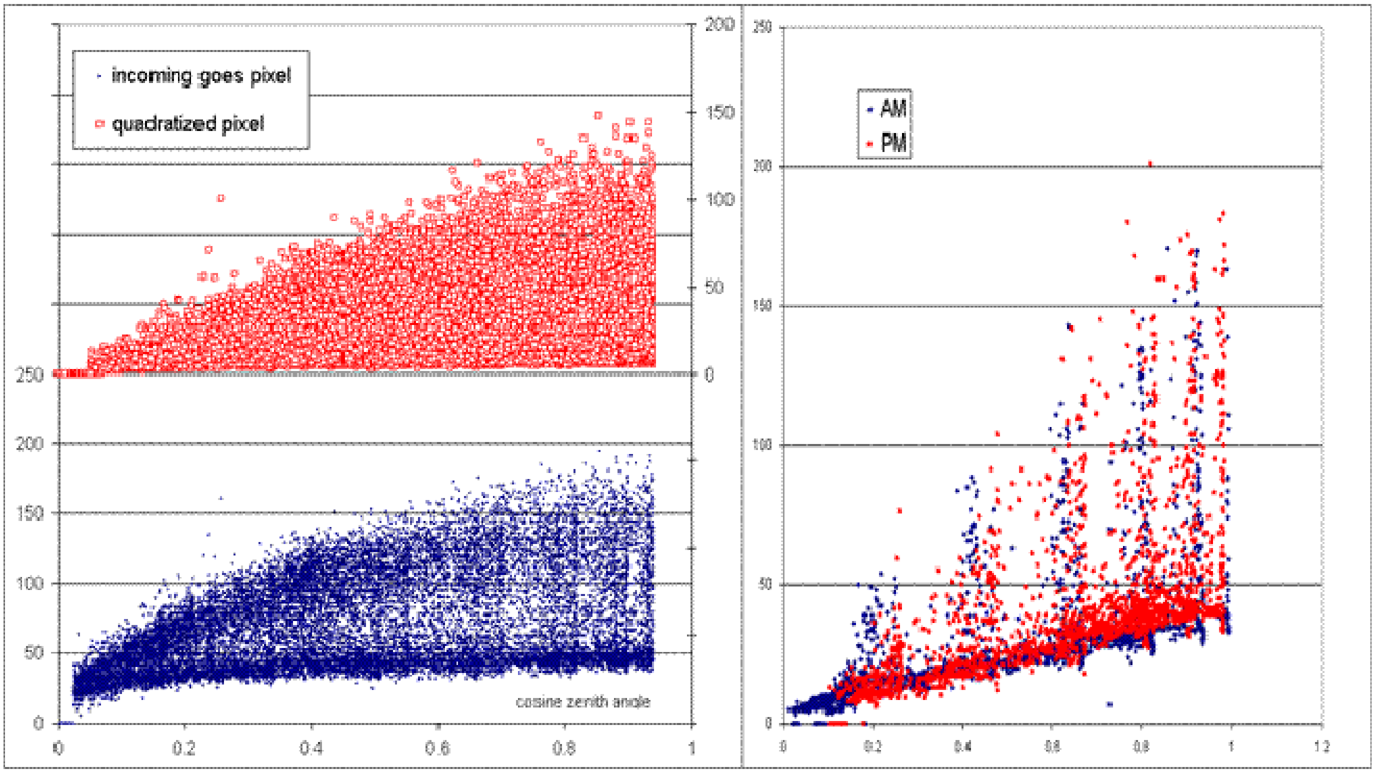

Figure 2: *Incoming GOES pixels (bottom left) exhibit a curved signature when plotted against the cosine of the zenith angle, Z. The pixels must be processed with a quadratic filter to exhibit the expected linear response to Cos Z (top left). A sample of incoming Meteosat 5 pixels (right) shows that incoming pixels are already linearly related to Cos Z and do not need to be modified before modeling.*

<u>Satellite calibration drift</u>: As explained in [1], the relative satellite sensor calibration is determined by observing the signature of solar-geometry-corrected pixels' time series at a given location (the model does not require absolute satellite calibration). Relative calibration is needed to properly specify the model's dynamic range's upper bound.

Compared to GOES, the Meteosat calibration drift over the considered period is minimal as shown in Figure 3. This is likely because onboard sensors typically exhibit exponential response decay over time. The new GOES sensors decay rapidly initially, while the older Meteosat 5 launched in 1991, has nearly reached a plateau in this respect.

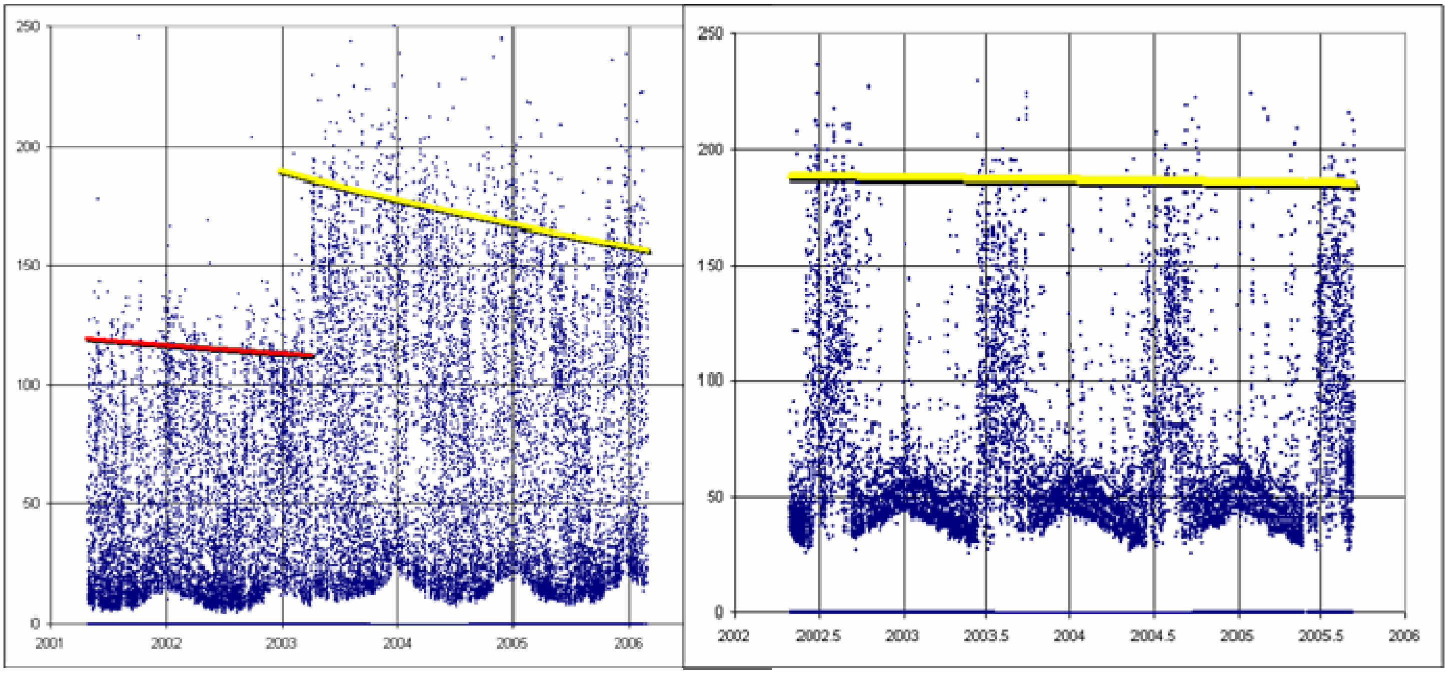

Figure 3 *-- Comparing normalized pixels at one location for GOES-east (left) and Meteosat (right). The solid lines represent the model's dynamic range upper bound. Note the change in satellite from GOES-8 to GOES-12 in early 2003 and the pronounced sensor's response exponential decay of GOES-12. Some decay is apparent in Meteosat, but it is minimal for the considered period [late in the life of the satellite which was launched for operation over Europe in 1991]. The point selected to illustrate Meteosat is near the southern Pakistan-India border. This region is characterized by a strong monsoon regime, hence the very distinct winter-summer trend (clouds in summer and clear in winter).*

Model Implementation

The satellite model involves three key processes and has been thoroughly described in the literature [1, 2]. The main modeling steps are summarized below, including adjustments and settings used for this project.

(1) <u>The model per se that relates pixel brightness to irradiance by comparing the local brightness' dynamic range to incoming pixels.</u> Each incoming pixel has its own dynamic range, specified from a 60-day trailing window and defining its lowest bound as the average of the 10 lowest values, unless there is new presence of snow on the ground, when the trailing window is shortened to two days and allowed to grow back to 60 days proceeding forward.

(2) <u>The calibration of the model to clear sky conditions</u>. This process was introduced to account for the rapid changes in ground albedo often observed in

arid conditions, and in particular, time-of-day variations caused by specular reflectivity of the ground. In this process the model insures that the "***n**^th^*" value at a given hour in a given month reaches the clear sky condition value. The *nth* ranking is a function of expected clearness conditions, varying from 1 for cloudy periods/locations to 6-7 for the driest periods/locations – the n^{th} ranking was estimated from the CSR model runs

(3) The correction of singularities due to complex albedo patterns. In this process, monthly maps of GHI and DNI are produced, and any instances where the pixel-to-pixel variation exceeds a given threshold are corrected by averaging neighboring pixels. Any pixel thus corrected is assigned a new clearness index kt'. The old minus new delta-kt' is then used as an input to the Time Series Generator (TSG) program that creates a new time series for that pixel. The new time series conserves the temporal patterns of the original time series, but increases/decreases the monthly averaged clearness index as needed, by applying the changes preferably to intermediate conditions.

RESULTS

Time series and monthly averaged, DNI and GHI

Hourly time series of global and direct irradiance were generated for the entire area analyzed, including a total of 30,000 pixels within Afghanistan, Pakistan and the neighboring countries within the field of view analyzed.

The hourly time series were processed into gridded monthly averages (e.g., see example for 2004) in figure 4.

All data were posted for download and further processing by the NREL team.

Final processing at NREL, comparison with other methods

The high resolution data produced at U. Albany are included in the final resource package and data toolkits developed at NREL. The resource package includes solar, wind and hydropower and biomass resource data.

Two other solar data sets are included in the NREL package in addition to the high resolution data prepared here. These are the NASA SSE data [7], and the NREL CSR data [8]. The former has a resolution of 1^{o} latitude-longitude (~ 100 Km at the ground) and is produced by NASA via processing of ISCCP data [9] – the SSE data are directly linked to the RetScreen renewable energy analysis package. NREL's CSR data have a resolution of ~ 40 km and are derived from cloud cover data assembled by the US Air force for the entire planet and derived from multiple sources, including satellite data, for the years 1985 through 1991.

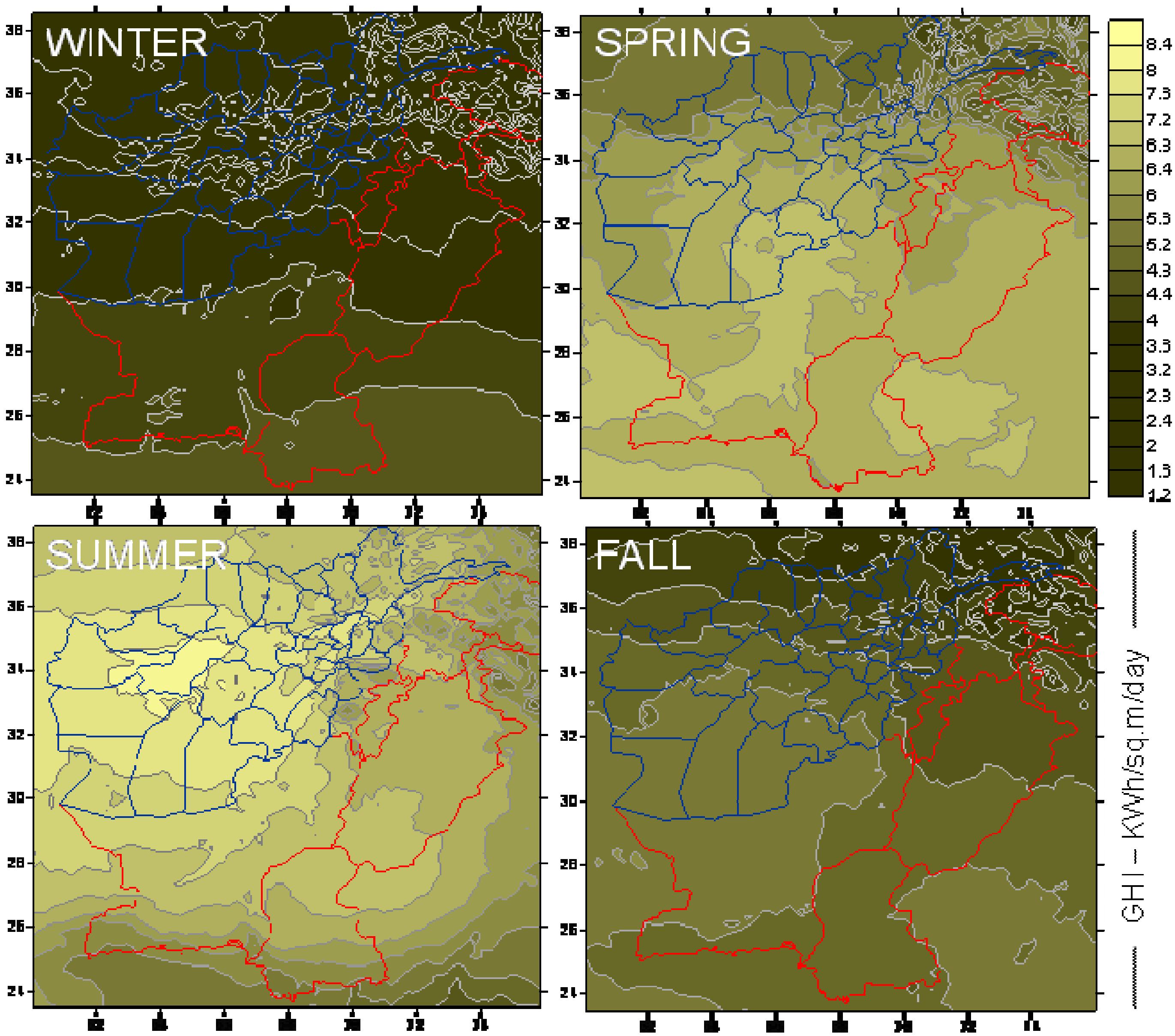

Figure 4: *Example of the data processed at U. Albany: Seasonal GHI for the year 2004*

The SSE and CSR solar data sets are used as a measure of quality control for the present high resolution data. As seen in Figures 5 and 6 and 7, the SUNY high resolution data lie about halfway between the CSR and SSE estimates. Although no ground measurements of high quality could be located, the fact that the high resolution data lies between estimates obtained by totally independent data sources and methodologies should increase regional confidence in the SUNY model which had otherwise been thoroughly validated for diverse climatic environments in its GOES-based version.

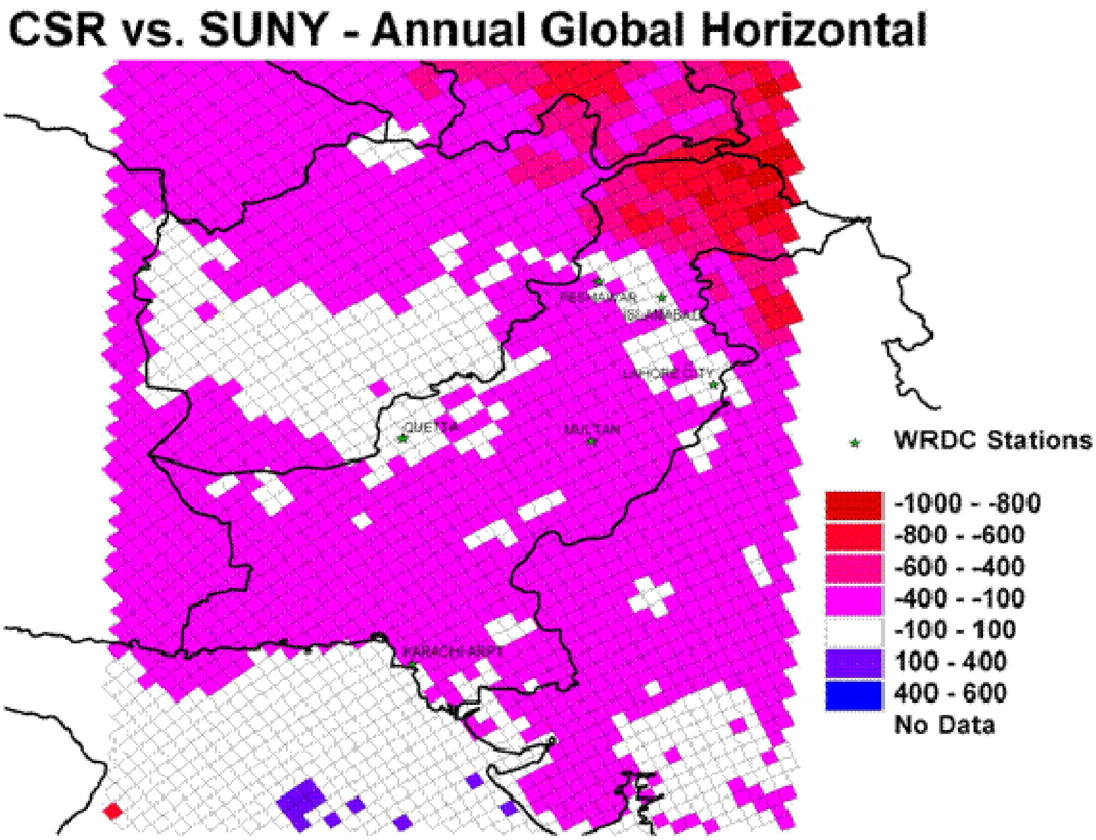

Figure 5: *Difference between the SUNY model and the NREL CSR Model for global horizontal irradiance. The SUNY model is slightly lower than the CSR model with more notable difference in the northeastern Pamir ranges.*

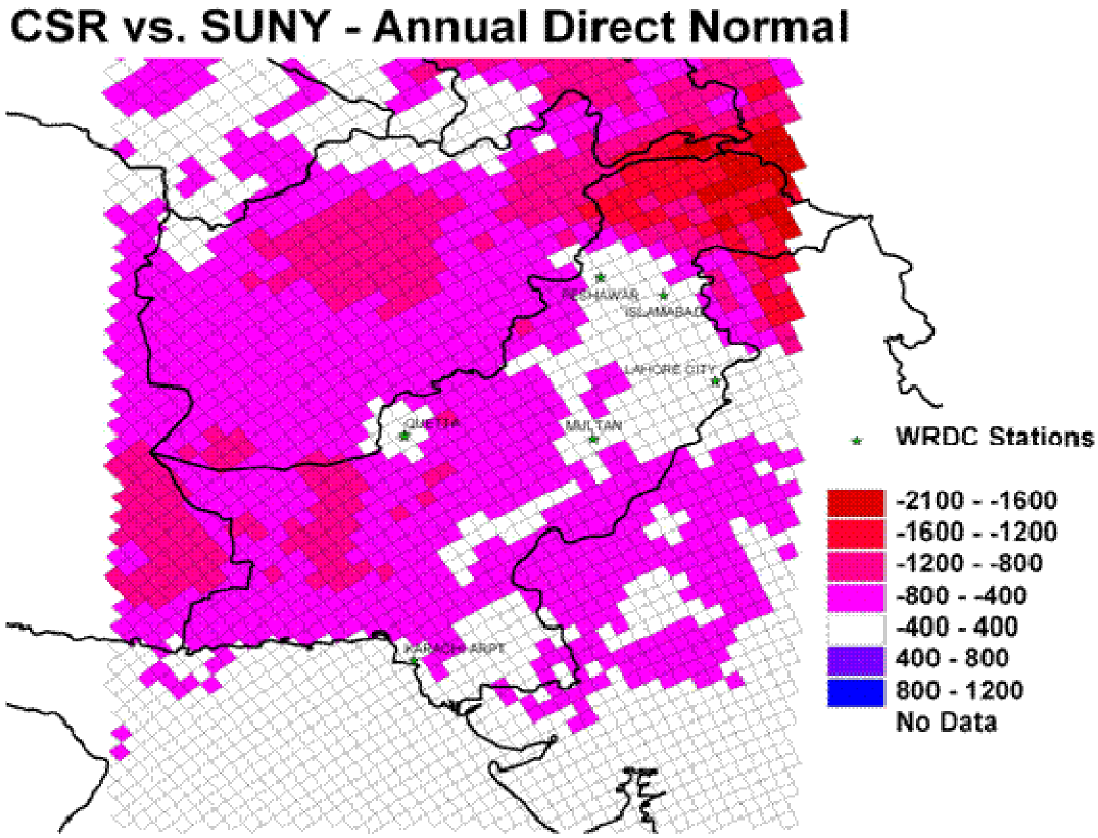

Figure 6: *Same as Figure 5, but for direct normal irradiance DNI.*

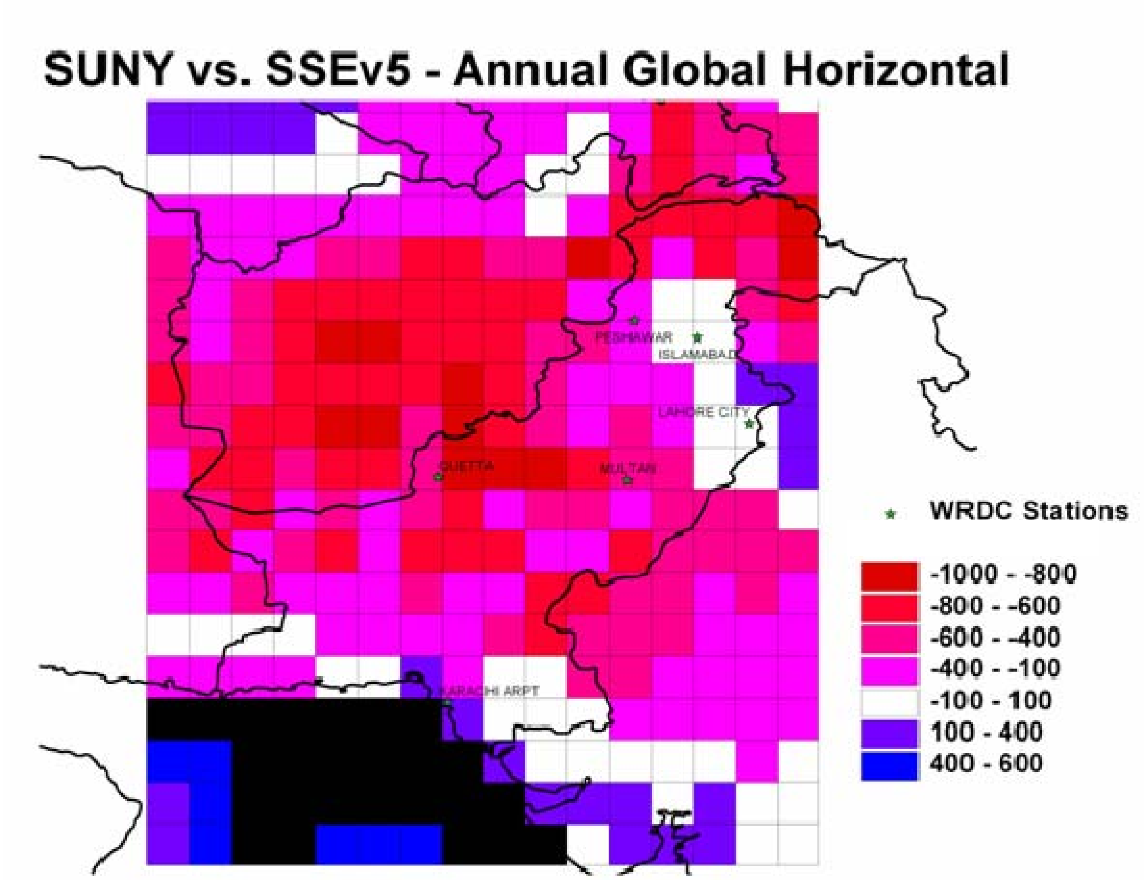

Figure 7: *Difference between the NASA-SSE and SUNY modeled GHI. The SUNY model is consistently higher than the NASA model, particularly in the highest irradiance locations of central Afghanistan. This observation is consistent with recent comparison between the two methodologies for the arid southwestern US.*

REFERENCE

1. Perez R., P. Ineichen, K. Moore, M. Kmiecik, C. Chain, R. George and F. Vignola, (2002): A New Operational Satellite-to-Irradiance Model. Solar Energy 73, 5, pp. 307-317.

2. Perez R., P. Ineichen, M. Kmiecik, K. Moore, R. George and D. Renne, (2004): Producing satellite-derived irradiances in complex arid terrain. Solar Energy 77, 4, 363-370

3. NOAA-NESDIS (2002-2005) Graphical Products: Operational Daily Snow Cover Analysis http://www.ssd.noaa.gov/PS/SNOW/

4. Zelenka, A. (1999): Personal Communication

5. Cano, D., J.M. Monget, M. Aubuisson, H. Guillard, N. Regas and L. Wald, (1986): A Method for the Determination of Global Solar Radiation from Meteorological Satellite Data. Solar Energy 37, pp. 31-39

6. Man Computer interactive Data Access System (McIdas): (2002-2005). Space and Science Engineering Center, University of Wisconsin

7. NASA Surface meteorology and Solar Energy Data Set http://eosweb.larc.nasa.gov/sse/RETScreen/

8. Maxwell, E. L. R. L. George and S. M. Wilcox, (1998): A Climatological Solar Radiation Model. Proc. 1998 ASES Conference Albuquerque, NM pp. 505-510.

9. ISCCP - International Satellite Cloud Climatology Project http://isccp.giss.nasa.gov/